© 2018 IEEE. Personal use of this material is permitted. Permission from IEEE must be obtained for all other uses, in any current or future media, including reprinting/republishing this material for advertising or promotional purposes, creating new collective works, for resale or redistribution to servers or lists, or reuse of any copyrighted component of this work in other works.

Reducing the Number of Elements in the Synthesis of a Broadband Linear Array with Multiple Simultaneous Frequency-Invariant Beam Patterns

Yanhui Liu, *Member, IEEE*, Juan Cheng, Kai Da Xu, *Member, IEEE*, Shiwen Yang, *Senior Member, IEEE*, Qing Huo Liu, *Fellow, IEEE*, and Y. Jay Guo, *Fellow, IEEE*

***Abstract*—The problem of reducing the number of elements in a broadband linear array with multiple simultaneous cross-over frequency-invariant (FI) patterns is considered. Different from the single FI pattern array case, every element channel in the multiple FI pattern array is divided and followed by multiple finite-impulse-response (FIR) filters, and each of the multiple FIR-filters has a set of coefficients. In this situation, a collective filter coefficient vector and its energy bound are introduced for each element, and then the problem of reducing the number of elements is transformed as minimizing the number of active collective filter coefficient vectors. Additionally, the radiation characteristics including beam-pointing direction, mainlobe FI property, sidelobe level and space-frequency notching requirement for each of the multiple patterns can be formulated as multiple convex constraints. The whole synthesis method is implemented by performing an iterative second-order cone programming (SOCP). This method can be considered as a significant extension of the original SOCP for synthesizing broadband sparse array with single FI pattern. Numerical synthesis results show that the proposed method by synthesizing multiple discretized cross-over FI patterns can save more elements than the original iterative SOCP by using a single continuously scannable FI pattern for covering the same space range. Moreover, even for multiple FI-patterns case with complicated space-frequency notching, the proposed method is still effective in the reduction of the number of elements.**

***Index Terms*—Broadband sparse array, multiple frequency-invariant (FI) beam patterns, space-frequency notching, iterative second-order cone programming (SOCP)**

I. Introduction

BROADBAND arrays with frequency invariant (FI) patterns have received increased attention in recent years due to their capability of receiving broadband signals without waveform distortion [1]. The broadband FI arrays usually consist of multiple elements, each connected to an analog-to-digital (A/D) converter followed by a finite-impulse-response (FIR) filter. They can be roughly classified into two categories: a) one is the array with an adaptive FI pattern which corresponds to data-dependent FIR filter coefficients [2]-[4]; b) the other is the array with a fixed FI pattern which corresponds to data-independent filter coefficients [5]-[13]. Compared to the adaptive FI beamforming, the array with a fixed FI pattern does not require to successively evaluate data-dependent coefficients and is much more computationally efficient [14]. However, the array with a single fixed FI pattern is not suitable when multiple broadband signals come from different directions or the direction of the desired signal varies with time. Clearly, the array with multiple simultaneous FI pencil patterns pointing at different directions can overcome this problem. Such a technique allows for covering wide-angle space without loss of pattern directivity, and consequently improves the performance of target search and angle estimation significantly in some applications [15], [16].

In general, broadband FI arrays need to locate their elements with a spacing of half wavelength calculated at the highest frequency of interest, so as to avoid the presence of grating lobes. Hence, they may require a large number of elements to achieve the desired broadband FI pattern characteristics. Especially for the case of multiple simultaneous FI patterns, each element channel in the array should be divided and followed by multiple different FIR filters, and each filter consists of a set of FIR coefficients used to provide this channel with an appropriate frequency-dependent excitation for one of the desired FI patterns. In this situation, reducing the number of elements and the associated filters is very significant for lowering down the whole system's cost. In the literature, there have been many sparse array synthesis methods, in both narrow- and broad-band cases, such as in [17]-[23]. Among them, most of sparse array synthesis methods focus on the problem of suppressing the grating-lobe and sidelobe levels, and they, however, do not pay much attention to the problem of how to keep the broadband FI property. Nevertheless, several papers can be found in [24]-[29] for synthesizing broadband sparse arrays with FI response properties. Among them, the asymptotic theory-based method in [24] providing an analytical solution is the most efficient way of broadband FI pattern, but it cannot accurately control the sidelobe level

Manuscript received September 24, 2017. This work was supported in part by the Shenzhen Science and Technology Innovation Project under Grant No YCYJ20170307141315473 and in part by the Australian Research Council (ARC) Discovery Project (DP) under Grant 160102219. (Corresponding author: Kai Da Xu).

Y. Liu is with the Shenzhen Research Institute of Xiamen University, Shenzhen 518057, China, and also with the Global Big Data Technologies Centre, University of Technology Sydney (UTS), NSW 2007, Australia (email: yanhui.liu@uts.edu.au).

J. Cheng and K. D. Xu are with Department of Electronic Science, Xiamen University, Fujian 361005, China, and also with the Shenzhen Research Institute of Xiamen University, Shenzhen 518057, China (kaidaxu@xmu.edu.cn).

S. Yang is with the School of Electronic Engineering, University of Electronic Science and Technology of China, Sichuan 610054, China (swnyang@uestc.edu.cn).

Q. H. Liu is with the Department of Electrical and Computer Engineering, Duke University, Durham, NC 27708, USA (qhliu@duke.edu).

Y. Jay Guo is with the Global Big Data Technologies Centre, University of Technology Sydney (UTS), NSW 2007, Australia (jay.guo@uts.edu.au).

and null region. The compressive sensing-based method in [27], [28] as well as the generalized matrix pencil method (GMPM) in [29], [30], give the synthesis result by matching it to a reference field pattern with preset amplitude and phase distributions. Such a way may lead to reduction of possible solution space and inaccurate control on the broadband sidelobe distribution. Especially when a complicated space-frequency notching is required in the synthesized broadband pattern, they would be not applicable. In addition, most of these methods synthesize only single FI pattern pointing at a certain direction. It's unclear whether they can be extended to deal with the currently concerned problem of synthesizing a sparse array with multiple simultaneous FI patterns since the best element positions usually change with different FI pattern requirements.

Recently, we presented a sparse broadband FI pattern array synthesis method based on the iterative second-order cone programming (SOCP) [31]. In this method, the problem of synthesizing a sparse array with a single FI pattern is transformed as solving a sequence of reweighted ℓ_1 optimizations under multiple convex constraints, and the broadband pattern characteristics including FI property, sidelobe level and null region can be accurately controlled without the requirement of a reference field pattern. The synthesized broadband sparse array can have continuous beam-scanning capability that has been shown in [31], but this is achieved at the cost of reducing the averaged inter-element spacing and increasing the number of elements. In this work, we will show that this method can be further extended to reduce the number of elements for synthesizing multiple cross-over FI patterns with accurate sidelobe control. The best common element positions can be chosen for simultaneously meeting multiple FI patterns by appropriately incorporating collective filter energy constraints in the synthesis procedure, and consequently the number of required elements can be less than the one obtained by synthesizing a continuously scannable FI pattern for the same angle-space coverage. In addition, complicated space-frequency notching can be added to each of the synthesized multiple FI patterns, which is very useful for applications where powerful interference sources arise in a certain space range and frequency band.

II. Formulation and Algorithm Implementation

A. Multiple FI pattern linear array model

Consider a linear antenna array composed of N isotropic elements which locate at $\boldsymbol{x} = [x_1, x_2, \cdots, x_N]$. To simultaneously produce M broadband FI focused patterns, each antenna channel of this array is divided and then connected to M digital finite-impulse-response (FIR) filters that are used to provide multiple frequency-dependent excitations for different patterns. Fig. 1 shows its beamforming network. For the mth $(m = 1, 2, \ldots, M)$ pattern, the array pattern is given by

$$p^{(m)}(\omega, \theta) = \sum_{n=1}^{N} \sum_{l=0}^{L-1} h_{l,n}^{(m)} a_n(\omega, \theta) e^{-j\omega l T_s} e^{-j\omega \tau_n(\theta)} \quad (1)$$

where $\omega = 2\pi f$ is the angle frequency, T_s is the temporal sampling interval, $h_{l,n}^{(m)}$ denotes the lth coefficient of the

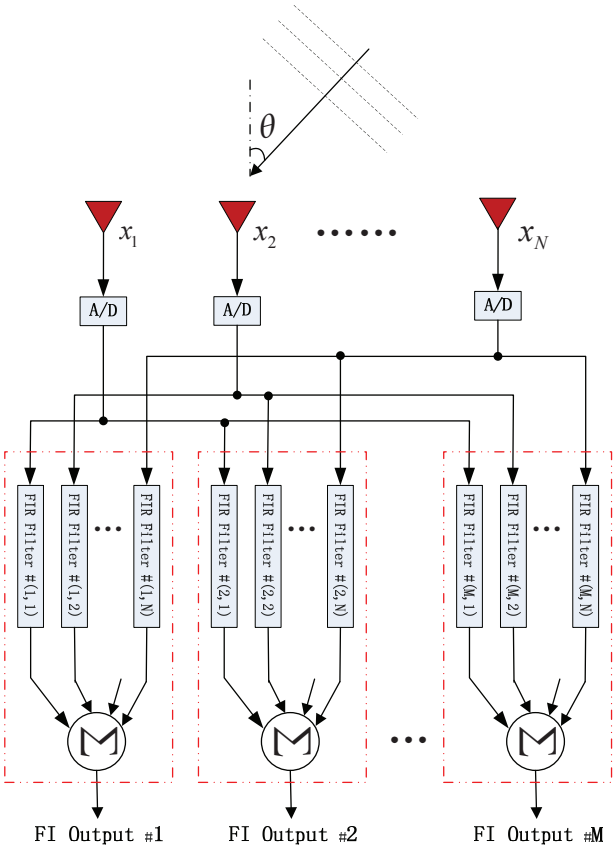

Fig. 1. Beamforming network for a unequally spaced linear array with multiple simultaneous FI patterns

mth filter (corresponding to the mth pattern) for the nth element, and L is the number of coefficients for each FIR filter. $\tau_n(\theta) = x_n \sin\theta / c$ is the time delay between the nth element and the zero-phase reference point, where θ is the wave propagation direction measured from the array broadside and c is the propagation velocity in the medium. $a_n(\omega, \theta)$ denotes the broadband element pattern for the nth element. Generally speaking, $a_n(\omega, \theta)$ is frequency-dependent and also varies among different antenna elements due to mutual coupling and platform effect. However, for simplicity in discussion on sparse antenna synthesis problems, here we assume that all the elements have the same element patterns without frequency-independence. That is, we assume $a_n(\omega, \theta) = a(\theta)$ for $n = 1, 2, \cdots, N$. Then, we rewrite (1) in the form of matrix product:

$$p^{(m)}(\omega, \theta) = \boldsymbol{s}_t^T(\omega) \boldsymbol{H}^{(m)} \boldsymbol{s}_\tau(\omega, \theta) \quad (2)$$

where

$$\boldsymbol{s}_t(\omega) = [1, e^{-j\omega T_s}, \ldots, e^{-j\omega(L-1)T_s}]^T \quad (3)$$

$$\boldsymbol{s}_\tau(\omega, \theta) = a(\theta)[e^{-j\omega\tau_1(\theta)}, e^{-j\omega\tau_2(\theta)}, \ldots, e^{-j\omega\tau_N(\theta)}]^T \quad (4)$$

$$\boldsymbol{H}^{(m)} = [\boldsymbol{h}_1^{(m)}, \boldsymbol{h}_2^{(m)}, \ldots, \boldsymbol{h}_N^{(m)}] \quad (5)$$

$$\boldsymbol{h}_n^{(m)} = [h_{0,n}^{(m)}, h_{1,n}^{(m)}, \ldots, h_{L-1,n}^{(m)}]^T \quad (6)$$

Through vectorising (2), we obtain that

$$p^{(m)}(\omega,\theta)=\boldsymbol{s}^T(\omega,\theta)\boldsymbol{\hbar}^{(m)} \tag{7}$$

where $\boldsymbol{s}(\omega,\theta)=\boldsymbol{s}_\tau(\omega,\theta)\otimes\boldsymbol{s}_t(\omega)$, and $\boldsymbol{\hbar}^{(m)}=\text{vec}\{\boldsymbol{H}^{(m)}\}$. Here, $\otimes$ denotes the Kronecker matrix product, and $\text{vec}\{\cdot\}$ denotes the vectorization operator which stacks the columns of a matrix on top of each other.

B. Synthesis of a sparse array with multiple FI patterns under sidelobe control and space-frequency notching

We will show that the problem of synthesizing a sparse array with multiple simultaneous FI beam pattern can be formulated as performing a sequence of reweighted ℓ_1-norm optimizations under multiple convex constraints. For each of the required FI patterns, multiple constraints should be used to separately control the broadband pattern characteristics in different regions including the mainlobe $\Theta_{\text{ML}}^{(m)}$, sidelobe region $\Theta_{\text{SL}}^{(m)}$, and the look-direction $\theta_{\text{look}}^{(m)}$, where $m=1,2,\ldots,M$. In addition, the common space-frequency notching for the multiple FI beam patterns can be also produced if required in applications. However, since the best element positions are usually changed with the desired FI pattern characteristics, the main difficulty in the multiple FI pattern array synthesis problem is that one has to find the best common element positions for simultaneously satisfying different pattern requirements. In the following, we will at first present the multiple FI pattern constraints, and then introduce how to find the best common element positions with optimized filter coefficients.

The multiple FI pattern constraints are given as follows:

i) *Spatial response variation (SRV) constraint for each pattern:*

$$\frac{\int_\Omega g(\omega)|s^T(\omega,\theta)\boldsymbol{\hbar}^{(m)}-s^T(\omega_{\text{ref}},\theta)\boldsymbol{\hbar}^{(m)}|^2d\omega}{\int_\Omega g(\omega)d\omega}\le\varepsilon_{\text{ML}} \tag{8}$$

where $g(\omega)$ is a positive frequency-domain weighting function, Ω is the frequency range of interest, and ϵ_{ML} is a specified weighted mean squared error of the broadband response variation respect to its value at a reference angle frequency $\omega_{\text{ref}}\in\Omega$. Usually, $\omega_{\text{ref}}=\sqrt{\omega_{\min}\omega_{\max}}$ is chosen as suggested in [31], where $\omega_{\min}$ and $\omega_{\max}$ are the minimum and maximum angle frequency of interest, respectively. Note that the above constraint is usually applied to the mainlobe region $\theta\in\Theta_{\text{ML}}^{(m)}$ for the synthesized mth pattern.

ii) *Multiple beam direction constraints at the reference frequency:*

$$|\boldsymbol{s}^T(\omega_{\text{ref}},\theta)\boldsymbol{\hbar}^{(m)}|=1,\quad\text{for }\theta=\theta_{\text{look}}^{(m)}. \tag{9}$$

To avoid the mth beam direction deviating from the desired one, an additional constraint of $\partial|\boldsymbol{s}^T(\omega_{\text{ref}},\theta)\boldsymbol{\hbar}^{(m)}|/\partial\theta=0$ at $\theta=\theta_{\text{look}}^{(m)}$ can be used. This constraint can be further simplified as the following [31],

$$\frac{\partial\{Re[\boldsymbol{s}^T(\omega_{\text{ref}},\theta)]\}}{\partial\theta}\boldsymbol{\hbar}^{(m)}=0,\ \text{for }\theta=\theta_{\text{look}}^{(m)}. \tag{10}$$

iii) *Sidelobe constraint for each pattern:*

$$|\boldsymbol{s}^T(\omega,\theta)\boldsymbol{\hbar}^{(m)}|^2\le\Gamma_{\text{SL}}^{(m)},\quad\text{for }\omega\in\Omega\text{ and }\theta\in\Theta_{\text{SL}}^{(m)} \tag{11}$$

where $\Gamma_{\text{SL}}^{(m)}$ is the sidelobe level which is usually the same for different FI patterns. That is, $\Gamma_{\text{SL}}^{(m)}=\Gamma_{\text{SL}}$ for $m=1,2,\cdots,M$.

iv) *Space-frequency notching constraint:*

$$|\boldsymbol{s}^T(\omega,\theta)\boldsymbol{\hbar}^{(m)}|^2\le\Gamma_{\text{Notch}},\ \text{for }(\omega,\theta)\in\{\Omega_{\text{Notch}},\Theta_{\text{Notch}}\} \tag{12}$$

where $(\Omega_{\text{Notch}},\Theta_{\text{Notch}})$ is the space-frequency notching range that is usually the same for different FI patterns in practice.

All the above constraints can be formulated in the form of linear constraints or second-order cone (SOC) constraints, which will be shown later. Thus, if element positions of an array are determined, the multiple pattern synthesis problem can be easily solved by using convex optimization. However, as mentioned previously, since each antenna channel should be divided and followed by multiple FIR filters for generating simultaneous multiple patterns, the cost of the whole system is much higher than the single-pattern case. To lower the cost, the number of antenna channels should be reduced as much as possible. For the case of multiple-pattern arrays, one antenna channel can be discarded only if all the coefficients of the associated multiple FIR filters are simultaneously minimized to be zeros. Here we define a collective filter coefficient vector for each antenna channel. For the nth antenna channel, the collective filter coefficient vector is given by

$$\breve{\boldsymbol{h}}_n=\left\{[\boldsymbol{h}_n^{(1)}]^T,[\boldsymbol{h}_n^{(2)}]^T,\ldots,[\boldsymbol{h}_n^{(M)}]^T\right\}^T. \tag{13}$$

Then we introduce an auxiliary variable η_n to constrain the energy bound of each $\breve{\boldsymbol{h}}_n$ for $n=1,2,\cdots,N$. That is,

$$\eta_n\ge\left\|[\boldsymbol{h}_n^{(1)}]^T,[\boldsymbol{h}_n^{(2)}]^T,\ldots,[\boldsymbol{h}_n^{(M)}]^T\right\|_2. \tag{14}$$

With the help of the above constraints, we can transform the problem of synthesizing a sparse linear array with multiple FI beam patterns under various space-frequency constraints as solving a weighted ℓ_1-norm optimization problem:

$$\min_{\{\boldsymbol{h}_n^{(m)},\eta_n;|_{n=1,\cdots,N}^{m=1,\cdots,M}\}}\ \sum_{n=1}^N\alpha_n\eta_n$$
$$\text{Const.}\begin{cases}\eta_n\ge\left\|[\boldsymbol{h}_n^{(1)}]^T,[\boldsymbol{h}_n^{(2)}]^T,\ldots,[\boldsymbol{h}_n^{(M)}]^T\right\|_2,\\ \qquad(n=1,2,\cdots,N);\\ \frac{\int_\Omega g(\omega)|\boldsymbol{s}^T(\omega,\theta)\boldsymbol{\hbar}^{(m)}-\boldsymbol{s}^T(\omega_{\text{ref}},\theta)\boldsymbol{\hbar}^{(m)}|^2d\omega}{\int_\Omega g(\omega)d\omega}\le\varepsilon^{\text{ML}}(\theta)\\ \qquad\text{for }\omega\in\Omega,\theta\in\Theta_{\text{ML}}^{(m)}\quad(m=1,2,\cdots,M);\\ |\boldsymbol{s}^T(\omega_{\text{ref}},\theta)\boldsymbol{\hbar}^{(m)}|=1\text{ and }\frac{\partial\{Re[\boldsymbol{s}^T(\omega_{\text{ref}},\theta)]\}}{\partial\theta}\boldsymbol{\hbar}^{(m)}=0,\\ \qquad\text{for }\theta=\theta_{\text{look}}^{(m)}\quad(m=1,2,\cdots,M);\\ |\boldsymbol{s}^T(\omega,\theta)\boldsymbol{\hbar}^{(m)}|^2\le\Gamma_{\text{SL}}^{(m)},\ \text{for }\omega\in\Omega,\theta\in\Theta_{SL}^{(m)}\\ \qquad(m=1,2,\cdots,M);\\ |\boldsymbol{s}^T(\omega,\theta)\boldsymbol{\hbar}^{(m)}|^2\le\Gamma_{\text{Notch}},\ (\omega,\theta)\in\{\Omega_{\text{Notch}},\Theta_{\text{Notch}}\}\\ \qquad(m=1,2,\cdots,M)\end{cases} \tag{15}$$

In the above, α_n $(n=1,2,\cdots,N)$ are weight coefficients for the weighted ℓ_1-norm optimization. As is well known, the

weighted ℓ_1-norm optimization can be iteratively implemented by appropriately updating the weight coefficients α_ns. Usually, at the initial iteration, the coefficients α_ns are chosen to be ones, and in this situation the weighted ℓ_1-optimization becomes a regular ℓ_1 optimization. Then, at the kth iteration, we can choose $\alpha_n^{(k)} = 1/(\eta_n^{(k-1)} + \delta)$ where δ is a small positive number and $\eta_n^{(k-1)}$s are results obtained from the $(k-1)$th weighted ℓ_1-norm optimization. The whole iteration procedure will proceed until the specified maximum iteration number is reached or the solution maintains unchanged multiple times. It has been shown that such an iterative weighted ℓ_1-norm can produce a closer approximation to ℓ_0-norm optimization and usually leads to a more sparse solution than the regular ℓ_1-norm optimization [31], [32].

C. SOCP-based algorithm implementation

In the proposed iterative synthesis procedure, each iteration needs to perform the weighted ℓ_1-norm optimization which can be solved by the second-order cone programming (SOCP). The general form of SOCP is given by [33]

$$\begin{aligned} &\max_{\boldsymbol{y}} \boldsymbol{b}^T \boldsymbol{y} \\ &\text{subject to } \boldsymbol{c_i} - \boldsymbol{A_i y} \in \text{SOC}^{C_i}, \quad i = 1, 2, \cdots, I. \end{aligned} \tag{16}$$

Here, all vectors and matrices are real-valued, $\boldsymbol{y}$ is a vector containing the design variables, I is the number of SOC constraints. The ith SOC constraint is defined by

$$\text{SOC}^{C_i} \doteq \left\{ (z_1, \boldsymbol{z_2}) \in \Re \times \Re^{(C_i - 1)} | z_1 \geq \|\boldsymbol{z_2}\| \right\}. \tag{17}$$

where z_1 is the first component of the vector $\boldsymbol{c_i} - \boldsymbol{A_i y}$, and $\boldsymbol{z_2}$ is the remains of that vector.

To formulate problem (15) as the form of (16), we at first define the optimization variable $\boldsymbol{y}$ as

$$\boldsymbol{y} = \{\boldsymbol{\eta}^T, [\boldsymbol{\hbar}^{(1)}]^T, [\boldsymbol{\hbar}^{(2)}]^T, \cdots, [\boldsymbol{\hbar}^{(M)}]^T\}^T \tag{18}$$

where $\boldsymbol{\eta} = [\eta_1, \eta_2, \cdots, \eta_N]^T$. As mentioned previously, η_n denotes the auxiliary variable for constraining the energy of all the filter coefficients for the nth antenna channel, and $\boldsymbol{\hbar}^{(m)}$ represents the vectorized vector of all the coefficients at different antennas for the mth pattern. Then the filter energy constraint of (14) can be transformed as

$$\boldsymbol{c}^{\text{Aux}} - \boldsymbol{A}^{\text{Aux}} \boldsymbol{y} \in \text{SOC}^{ML+1}, \tag{19}$$

for $n = 1, 2, \cdots, N$, where

$$\boldsymbol{c}^{\text{Aux}} = \boldsymbol{0}_{(ML+1)\times 1} \tag{20}$$

and

$$\boldsymbol{A}^{\text{Aux}} = \begin{bmatrix} -\boldsymbol{v}_n^T & \boldsymbol{0}_{1\times MNL} \\ \boldsymbol{0}_{ML\times N} & -\boldsymbol{I}_{M\times M} \bigotimes \{\boldsymbol{v}_n^T \bigotimes \boldsymbol{I}_{L\times L}\} \end{bmatrix} \tag{21}$$

In the above, $\boldsymbol{I}_{M\times M}$ and $\boldsymbol{I}_{L\times L}$ are diagonal matrices, and $\boldsymbol{v}_n^T$ is the nth column of a diagonal matrix $\boldsymbol{I}_{N\times N}$. $\boldsymbol{I}_{M\times M} \bigotimes \{\boldsymbol{v}_n^T \bigotimes \boldsymbol{I}_{L\times L}\}$ is used to pick out the collective filter coefficient vector $\boldsymbol{h}_n$ for the nth antenna channel from the optimization vector y.

To implement all the pattern constraints, we need to sample the angle frequency ω and spatial variable θ. Assume that the sampled frequencies are $\{\omega_p \in \Omega; |p = 0, 1, \cdots, P-1\}$, and the sampled angles are $\{\theta_q \in \Theta; |q = 0, 1, \cdots, Q-1\}$. For the mth pattern, θ_q may belong to either $\Theta_{\text{ML}}^{(m)}$ or $\Theta_{\text{SL}}^{(m)}$, otherwise $(\omega_p, \theta_q) \in \{\Omega_{\text{Notch}}, \Theta_{\text{Notch}}\}$ for the notching region case. For the SRV constraint of (8), at each $\theta_q \in \Theta_{\text{ML}}^{(m)}$, we obtain that

$$\boldsymbol{c}^{\text{ML}} - \boldsymbol{A}^{\text{ML}} \boldsymbol{y} \in \text{SOC}^{2J+1}, \quad \text{for each of} \tag{22}$$

where

$$\boldsymbol{c}^{\text{ML}} = [\sqrt{\varepsilon_{\text{ML}}}, \boldsymbol{0}_{1\times 2J}]^T \tag{23}$$

and

$$\boldsymbol{A}^{\text{ML}} = \begin{bmatrix} \boldsymbol{0}_{1\times N} & \boldsymbol{0}_{1\times MNL} \\ \boldsymbol{0}_{1\times N} & \boldsymbol{v}_m^T \bigotimes Re\{\boldsymbol{s}^T(\omega_{\text{ref}}, \theta_q) - \boldsymbol{s}^T(\omega_0, \theta_q)\} \\ \boldsymbol{0}_{1\times N} & \boldsymbol{v}_m^T \bigotimes Im\{\boldsymbol{s}^T(\omega_{\text{ref}}, \theta_q) - \boldsymbol{s}^T(\omega_0, \theta_q)\} \\ \vdots & \vdots \\ \boldsymbol{0}_{1\times N} & \boldsymbol{v}_m^T \bigotimes Re\{\boldsymbol{s}^T(\omega_{\text{ref}}, \theta_q) - \boldsymbol{s}^T(\omega_{P-1}, \theta_q)\} \\ \boldsymbol{0}_{1\times N} & \boldsymbol{v}_m^T \bigotimes Im\{\boldsymbol{s}^T(\omega_{\text{ref}}, \theta_q) - \boldsymbol{s}^T(\omega_{P-1}, \theta_q)\} \end{bmatrix} \tag{24}$$

where $\boldsymbol{v}_m$ is the mth column of the diagonal matrix $\boldsymbol{I}_{M\times M}$ and it is used to pick out the single $\boldsymbol{\hbar}^{(m)}$ for the mth pattern from the whole vector $\boldsymbol{y}$. In addition, the sidelobe constraint of (11) can be transformed into the SOCP form as the following:

$$\boldsymbol{c}^{\text{SL}} - \boldsymbol{A}^{\text{SL}} \boldsymbol{y} \in \text{SOC}^3 \tag{25}$$

for each $\theta_q \in \Theta_{\text{SL}}^{(m)}$ at every $\omega_p \in \Omega$, where

$$\boldsymbol{c}^{\text{SL}} = [\sqrt{\Gamma_{\text{SL}}^{(m)}(\theta_q)}, \boldsymbol{0}_{1\times 2J}]^T \tag{26}$$

and

$$\boldsymbol{A}^{\text{SL}} = \begin{bmatrix} \boldsymbol{0}_{1\times N} & \boldsymbol{0}_{1\times MNL} \\ \boldsymbol{0}_{1\times N} & \boldsymbol{v}_m^T \bigotimes Re\{\boldsymbol{s}^T(\omega_p, \theta_q)\} \\ \boldsymbol{0}_{1\times N} & \boldsymbol{v}_m^T \bigotimes Im\{\boldsymbol{s}^T(\omega_p, \theta_q)\} \end{bmatrix} \tag{27}$$

Similarly, the space-frequency notching constraint of (12) can be transformed as

$$\boldsymbol{c}^{\text{Notch}} - \boldsymbol{A}^{\text{Notch}} \boldsymbol{y} \in \text{SOC}^3 \tag{28}$$

for each $(\omega_p, \theta_q) \in \{\Omega_{\text{Notch}}, \Theta_{\text{Notch}}\}$, where

$$\boldsymbol{c}^{\text{Notch}} = [\sqrt{\Gamma_{\text{Notch}}}, \boldsymbol{0}_{1\times 2J}]^T \tag{29}$$

and $\boldsymbol{A}^{\text{Notch}}$ has the same form of $\boldsymbol{A}^{\text{SL}}$ but with different (ω_p, θ_q). The multiple-beam direction constraint of (9) can be rewritten as

$$\boldsymbol{c}^{\text{look}} - \boldsymbol{A}^{\text{look}} \boldsymbol{y} \in \text{SOC}^3 \tag{30}$$

for each beam direction $\theta = \theta_{\text{look}}^{(m)}$ at $\omega = \omega_{\text{ref}}$, where

$$\boldsymbol{c}^{\text{look}} = [0, 1, 0]^T \tag{31}$$

and

$$\boldsymbol{A}^{\text{look}} = \begin{bmatrix} \boldsymbol{0}_{1\times N} & \boldsymbol{0}_{1\times MNL} \\ \boldsymbol{0}_{1\times N} & \boldsymbol{v}_m^T \bigotimes Re\{\boldsymbol{s}^T(\omega_{\text{ref}}, \theta_{\text{look}})\} \\ \boldsymbol{0}_{1\times N} & \boldsymbol{v}_m^T \bigotimes Im\{\boldsymbol{s}^T(\omega_{\text{ref}}, \theta_{\text{look}})\} \end{bmatrix} \tag{32}$$

The derivative constraint of (10) can be similarly reformulated.

Finally, the objective function of problem (15) can be easily written as the form of (16) by defining

$$\boldsymbol{b} = -[\alpha_0^k, \alpha_1^k, \cdots, \alpha_{N-1}^k, \boldsymbol{0}_{1\times MNL}]^T \tag{33}$$

Note that the whole optimization process in (15) needs to sequentially perform the SOCP solver, but all the matrices and vectors defined above are fixed at each iteration except that the vector $\boldsymbol{b}$ needs to be updated at each iteration. Several optimization toolboxes for solving the SOCP problem are available, and in this work we used the SeDuMi (Self-Dual-Minimization) tool [33].

III. Numerical Results

In this section, we will carry out several numerical synthesis experiments to validate the effectiveness of the proposed method for reducing the number of elements in the synthesis of multiple simultaneous FI beam patterns. In all the following experiments, we choose $g(\omega) = 1$ and $\omega_{\text{ref}} = \sqrt{\omega_{\min}\omega_{\max}}$, and set $\varepsilon_{ML} = 4 \times 10^{-4}$ at the angle of each pattern mainlobe where the FI property should be kept. Besides, we adopt $\delta = \max\{\eta_n^0\}/10^5$ in the iterations, where η_n^0s $(n = 0, 1, \cdots, N-1)$ are obtained from the initial iteration. It should be noted that although all the parameters are chosen similarly as used in [31], the proposed method deals with the multiple FI pattern synthesis problem which cannot be solved by the original SOCP synthesis method in [31].

A. Comparative study on synthesizing multiple cross-over FI patterns and a continuously scannable FI pattern

In the first example, we apply the proposed method to synthesize a sparse linear array with multiple cross-over FI beam patterns covering a specified spatial angle range. Assume that the array has isotropic elements. That is, $a(\theta) = 1$. To evaluate the performance of the proposed method for different space coverage ranges, we consider four different cases: $\pm 16.25^\circ$, $\pm 32.5^\circ$, $\pm 48.75^\circ$ and $\pm 61.75^\circ$ space coverage ranges. For the proposed method, we assume that they are covered by 5, 10, 15 and 19 FI beam patterns, respectively, and all the FI beams are separated with an interval of 6.5°. The FI property for each beam pattern is maintained within about 10° mainlobe region over the frequency band of interest from 0.3 to 0.6 GHz. Choose an initial linear array with 117 potential antenna elements with a uniform spacing of $\lambda_U/8$ where λ_U is the wavelength at 0.6 GHz, and the total aperture is $14.5\lambda_U$. The channel for each element is divided into multiple sub-channels and then followed by multiple FIR filters (the number of filters for each channel is equal to the number of FI patterns), each with $L = 20$ and $T_s = 1/1.2$GHz. The desired sidelobe level (SLL) is set to be -14 dB over the frequency band of interest for each FI pattern. For comparison, the original iterative SOCP method in [31] which can obtain a sparse linear array with a continuously scannable FI pattern, is applied to this example with the same potential element positions and SLL configuration. In addition, the asymptotic theory-based design (ATD) method in [24] is also used to generate a continuously scannable FI pattern under the same beamwidth condition. Note that in the ATD method, since the element positions and excitations are analytically obtained using an asymptotic theory in the assumption of full-space scanning range, and they are exactly the same for different scanning range cases.

Table I shows the synthesis results of the three methods for different space coverage ranges (the element saving is calculated by comparing the obtained nonuniformly spaced array with a $0.5\lambda_U$-spaced array occupying the same aperture). Clearly, compared with the ATD method, both the original iterative SOCP and the proposed method not only have more accurate sidelobe control but also save more elements for all test cases except the case with the largest space coverage $\pm 61.75^\circ$. In addition, for covering the same angle range, the proposed method by using mutiple discretized cross-over FI beam patterns can in general save more elements than the original iterative SOCP by generating a single continuously scannable FI beam pattern except when the required coverage angle gets very wide. As an illustration, Fig. 2 shows the synthesized 15 cross-over FI beam patterns within $0.3 \sim 0.6$ GHz band for the case of $\pm 48.75^\circ$ space coverage using the proposed method (the obtained lowest cross-over level is about -2.8 dB within the whole frequency band of interest). In this case, 19 nonuniformly spaced elements are required. It is mentioned that both the original iterative SOCP and the ATD method requires 21 nonuniformly spaced elements for generating a continuously scannable FI pattern covering the $\pm 48.75^\circ$ space range, as shown in Table I. Fig. 3 shows the selected 19 elements from the potential 117 positions by the proposed method. The element saving in this case is 36.67%.

On the other hand, it should be noted that compared with the original SOCP method for the single FI beam pattern synthesis, the proposed method dealing with the simultaneous multiple FI beam pattern synthesis problem has extremely increased the computational burden because the number of optimization variables and the number of pattern constraints are increased by a factor of the beam number. For example, for the $\pm 48.75^\circ$ space coverage case, the total number of filter coefficients to be optimized is equal to $20 \times 117 \times 15 = 35100$. The time costs by the proposed method and the other two methods for all test cases are listed in the last column of Table I (all the tests are performed on a work station with Intel Xeon CPU E5-2697@2.30GHz). As can be seen, the proposed method is the most time consuming among the three methods. This can be considered as a necessary cost to obtain multiple simultaneous FI beam patterns. Besides, it should be mentioned that conventional stochastic optimization methods such as genetic algorithm and simulated annealing are basically not applicable due to the huge number of unknowns for the problems concerned.

B. Synthesizing multiple cross-over FI patterns with uniform SLL and one space-frequency notching

In this example, we will check the effectiveness of the proposed method for synthesizing multiple cross-over FI pattern with one common space-frequency notching. Such situation happens when some interference signals in a certain band come from outside of the required space coverage. Assume that we have the same potential element positions and FIR filter parameters as those used in the first example. That is, $N = 117$ and $d = \lambda_U/8$ for the potential elements, $L = 20$ and $T_s = 1/1.2$GHz for the FIR filters. We further assume

TABLE I
SYNTHESIS RESULTS OF THE PROPOSED METHOD, THE ORIGINAL ITERATIVE SOCP IN [31] AND THE ATD METHOD IN [24] ($L = 20$, $T_s = 1/1.2GHz$, SYN. APERTURE=$14.5\lambda_U$, N_s IS THE NUMBER OF SELECTED ELEMENTS)

Synthesis methods	Coverage range	N_s	Element saving	Spacing($/\lambda_U$)			$SLL_{\max}$ (dB)	Time
				Max	Min	Mean		
The proposed (Multi-beam synth.)	$[-16.25°, 16.25°]$	15	50%	2.250	0.6250	1.036	-13.92	0.4 days
	$[-32.50°, 32.50°]$	17	43.33%	2.250	0.5000	0.9063	-13.53	2.6 days
	$[-48.75°, 48.75°]$	19	36.67%	2.000	0.5000	0.8056	-13.63	13.7 days
	$[-61.75°, 61.75°]$	21	30%	1.750	0.5000	0.7250	-13.87	17.5 days
Original SOCP (Single-beam synth.)	$[-16.25°, 16.25°]$	17	43.33%	1.625	0.6250	0.9063	-13.92	17.0 mins
	$[-32.50°, 32.50°]$	19	36.67%	2.250	0.5000	0.8056	-13.78	20.2 mins
	$[-48.75°, 48.75°]$	21	30%	2.000	0.5000	0.7250	-13.86	22.4 mins
	$[-61.75°, 61.75°]$	21	30%	1.875	0.5000	0.7250	-13.84	25.7 mins
ATD method (Single-beam synth.)	$[-16.25°, 16.25°]$	21	30%	1.552	0.5000	0.7275	-14.29	2.1 sec
	$[-32.50°, 32.50°]$						-11.42	2.3 sec
	$[-48.75°, 48.75°]$						-11.08	2.5 sec
	$[-61.75°, 61.75°]$						-10.15	2.6 sec

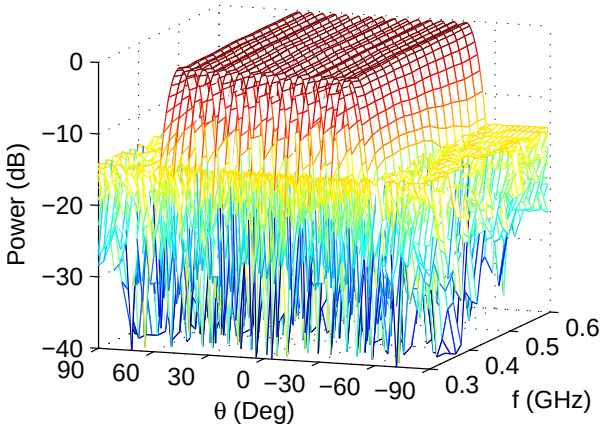

(a)

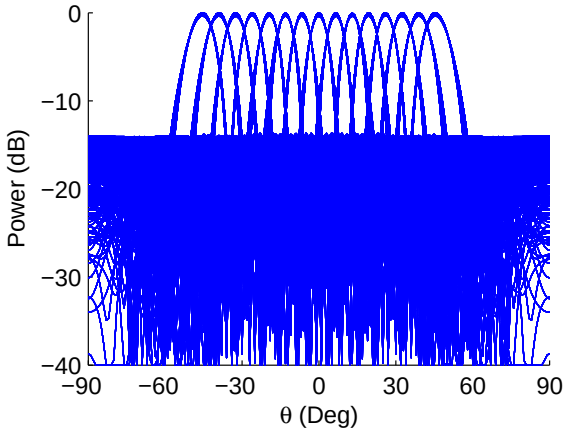

(b)

Fig. 2. The synthesized 15 cross-over FI beam patterns ($0.3 \sim 0.6$ GHz) covering the $\pm 48.75°$ angle space. (a) Joint space-frequency distribution,(b) patterns at 16 discrete frequencies.

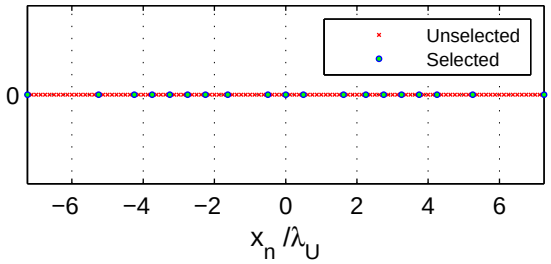

Fig. 3. The selected and unselected element positions for the 15 cross-over FI beam patterns in Fig. 2.

that 11 cross-over patterns within the same frequency band of $0.3 \sim 0.6$ GHz are required to cover a $\pm 33°$ space , with the beam interval of $6°$ (the obtained cross-over level would be higher than the one in the first example). The desired SLL is still -14 dB. Now, a -50 dB space-frequency notching is added to each FI pattern within the space range of $[-68°, -52°]$ and the frequency band of $[0.4, 0.6]$ GHz. Fig. 4 shows the synthesized 11 cross-over FI beam patterns by the proposed method. As can be seen, all the synthesized beam patterns still keep the FI property and the desired uniform SLL as expected. The lowest cross-over level is now about -1.8 dB in the frequency band of interest. In addition, the -50 dB pattern notching is accurately implemented within the required space-frequency region. In this example, 19 elements are selected from the potential ones of the initial array. Fig. 5 shows the distribution of these element positions. The element saving is 36.67% in this case.

C. Synthesizing multiple cross-over FI patterns with uniform SLL and more complicated space-frequency notching

In the third example, we consider to synthesize a sparse array with multiple cross-over FI patterns and more complicated space-frequency notching requirement. Now assume that 10 cross-over FI patterns in $0.4 \sim 1$ GHz band are required to cover a $\pm 38°$ angle space, with the beam interval of $7.6°$. The desired sidelobe level is set to be less than -13.5 dB for each pattern in the frequency band of interest. For each FI pattern, two space-frequency notching regions are required: 1) the first is a -50 dB notching within the space range of $[-52°, -60°]$ and the whole frequency band of $[0.4, 1]$ GHz; 2) the second is a -53 dB notching within the space range of $[54°, 58°]$ and the frequency band of $[0.6, 0.8]$ GHz. Choose an initial linear array with 130 $\lambda_U/8$-spaced potential elements (the aperture is about $16.125\lambda_U$), and set $L = 16$ and $T_s = 1/2$GHz for the FIR filters. Fig. 6 shows the synthesized 10 cross-over FI beam

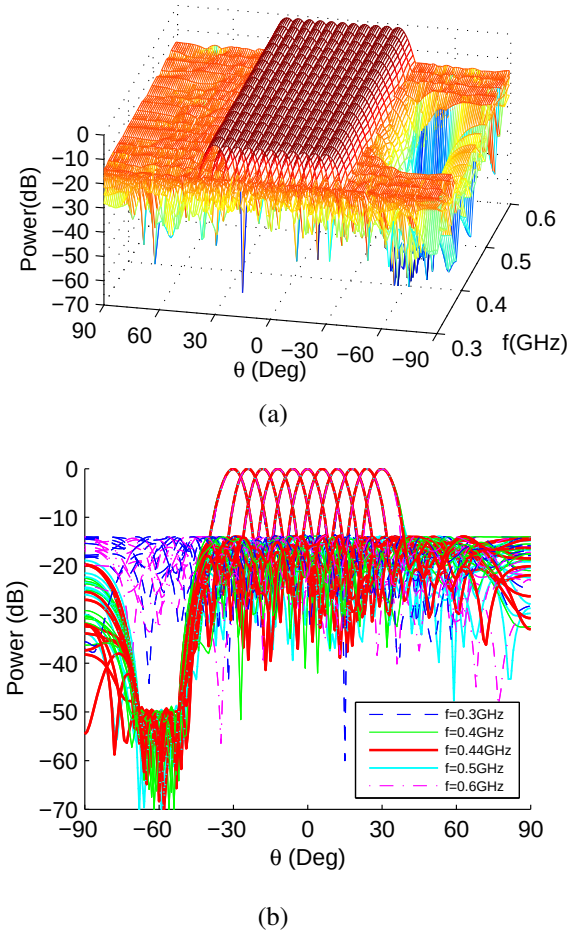

Fig. 4. The synthesized 11 cross-over FI beam patterns ($0.3 \sim 0.6$ GHz) covering the $\pm 33^\circ$ angle space. Each beam pattern is imposed with an additional -50 dB space-frequency notching within $[-68^\circ, -52^\circ]$ and $0.4 \sim 0.5$ GHz. (a) Joint space-frequency distribution, (b) patterns at the frequencies of $[0.3, 0.4, 0.44, 0.5, 0.6]$ GHz.

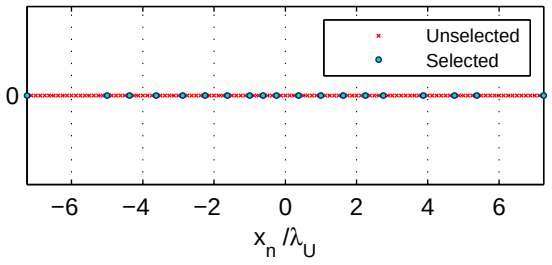

Fig. 5. The selected and unselected element positions for the 11 cross-over FI beam patterns with one space-frequency notching in Fig. 4.

patterns with the two space-frequency notching regions by the proposed method. As can be seen, even with so complicated multiple pattern requirement, the obtained broadband radiation characteristics including FI property, broadband SLL and the space-frequency notching performance for each pattern are still satisfactory. The lowest cross-over level between neighboring FI beams is about -3 dB within the frequency band of interest. Fig. 7 shows the selected and unselected elements

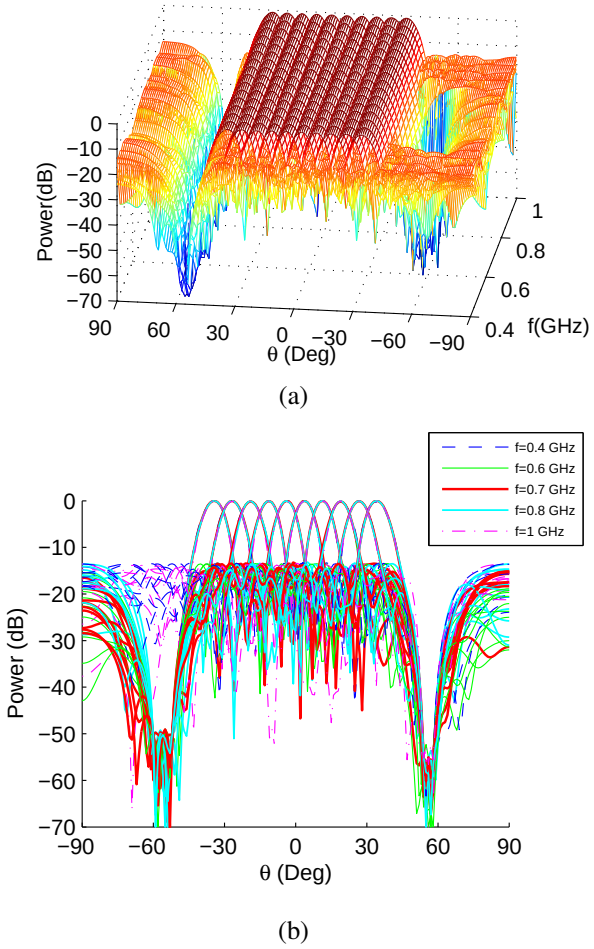

Fig. 6. The synthesized 10 cross-over FI beam patterns ($0.4 \sim 1$ GHz) covering the $\pm 33^\circ$ angle space. Each beam pattern is imposed with a -50 dB space-frequency notching within $[-52^\circ, -60^\circ]$ and $[0.4, 1]$ GHz and another -53 dB notching within $[54^\circ, 58^\circ]$ and $[0.6, 0.8]$ GHz. (a) Joint space-frequency distribution, (b) patterns at the frequencies of $[0.4, 0.6, 0.7, 0.8, 1]$ GHz.

for the synthesized array. As can be seen, 24 elements are now required due to the complicated notching requirement, and the element saving is about 27.27% in this example.

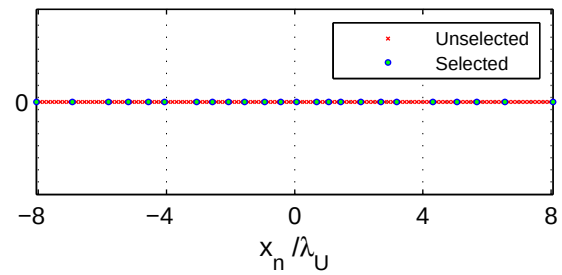

Fig. 7. The selected and unselected element positions for the 10 cross-over FI beam patterns with two space-frequency notching regions in Fig. 6.

D. Synthesizing multiple FI patterns with non-isotropic elements and quantization errors

In this example, we consider synthesizing a sparse array with multiple FI patterns in the case of non-isotropic elements. Assume that the array element has the angle dependence of $\cos\theta$. Now, we try to generate 11 cross-over FI beam patterns in a broad frequency band of $0.3 \sim 1$ GHz. The ratio of the highest to lowest frequency reaches about 3.3. The 11 FI beams in total cover a 44° angle space with an interval of 8°, and the desired SLL for each beam is set as -14 dB respect to the broadside beam gain. Choose the initial linear array with 113 $\lambda_U/8$-spaced potential elements (the aperture is $14\lambda_U$), and set $L = 20$ and $T_s = 1/2$GHz for the FIR filters. The synthesized 11 FI beam patterns are shown in Fig. 8. As can be seen, for each beam pattern, the obtained mainlobe maintains the FI property and the SLL meets the specification as well. This shows the robustness of the proposed method for the non-isotropic element case. In addition, it is observed that the obtained beam gain is reduced as the beam direction deviates from the broadside due to the element pattern modulation. The synthesized array has 14 selected elements, and the selected elements as well as unselected ones are shown in Fig. 9. In this example, we save about 50% elements if compared with an array with $\lambda_U/2$-spaced elements occupying the same aperture.

At last, let us consider something about implementing the obtained FI patterns. As an illustration, Fig. 10 shows the obtained FIR coefficients for producing the broadside FI beam pattern shown in Fig. 8. Fig. 11 shows the corresponding transfer functions including amplitude and phase frequency responses for the FIR filters for this pattern. Note that only 7 transfer functions are plotted since they are symmetrical about the array center for the broadside beam case. As can been seen, both the amplitude and phase frequency responses look different from conventional filter responses, and they would be not easy to implement if analog filters are used. Fortunately, we can use analog-to-digital convertors to sample the analog signals and implement the complicated frequency-responses in digital way. For the digital FIR filters, one thing we need to care about is the quantization of coefficients which will affect the accuracy of the realized coefficients and probably degrade the performance of the obtained FI beam pattern. Fig. 12(a) shows the original broadside FI beam pattern extracted from Fig. 8, and Fig. 12(b)-(d) show the realized patterns produced by the quantized coefficients with 5, 6 and 7 bits (all including one sign bit), respectively. As can be seen, the obtained FI beam pattern becomes more and more approaching to the original one as the length of quantization bits increases from 5 to 7. The original SLL is -13.86 dB while those for the quantized patterns with 5, 6 and 7 bits are -11.29, -11.70 and -13.52 dB, respectively. Similar phenomena are also observed for the scanned FI beam patterns. Fig. 13(a)-(d) show the original FI pattern and the patterns realized by quantized coefficients with 5, 6 and 7 bits (also including one sign bit) for the beam which is pointing at 40° with covering the space of $[36^\circ, 44^\circ]$. In this case, the original SLL is -14.11 dB while those for the quantized patterns with 5, 6 and 7 bits are -10.32, -11.98 and -13.05 dB , respectively. We can see that quantizing the FIR coefficients with 7 bits can maintain acceptable pattern performance in this example.

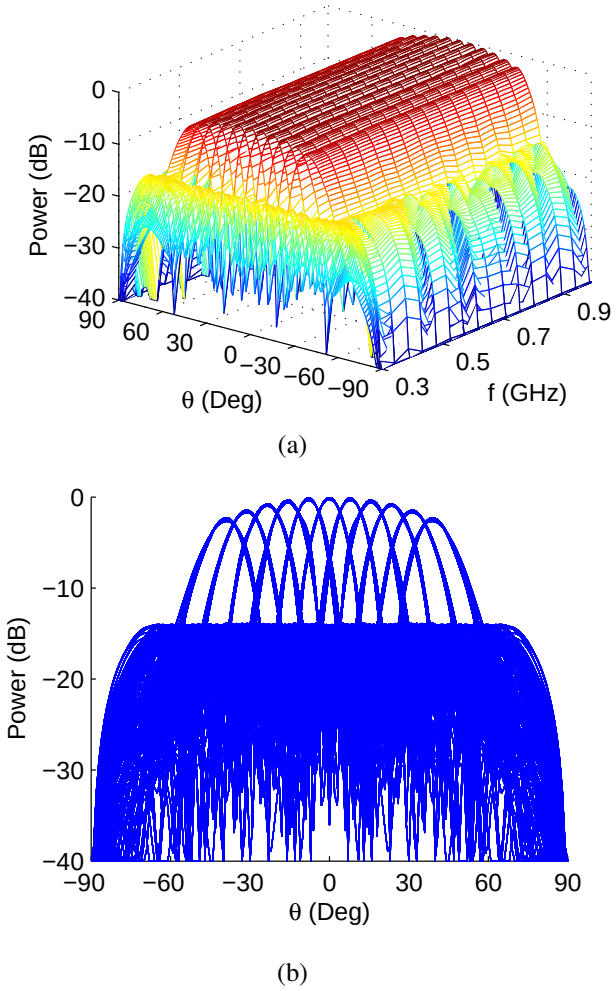

Fig. 8. The synthesized 11 cross-over FI beam patterns ($0.3 \sim 1$ GHz) covering the $\pm 44^\circ$ angle space. (a) Joint space-frequency distribution, (b) patterns at 16 discrete frequencies.

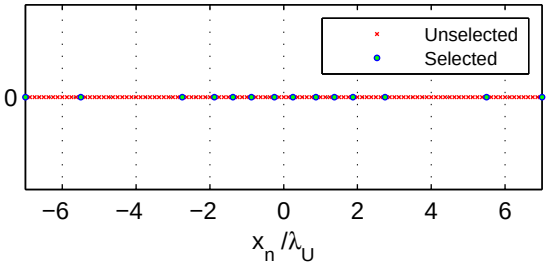

Fig. 9. The selected and unselected element positions for the 11 cross-over FI beam patterns shown in Fig. 8.

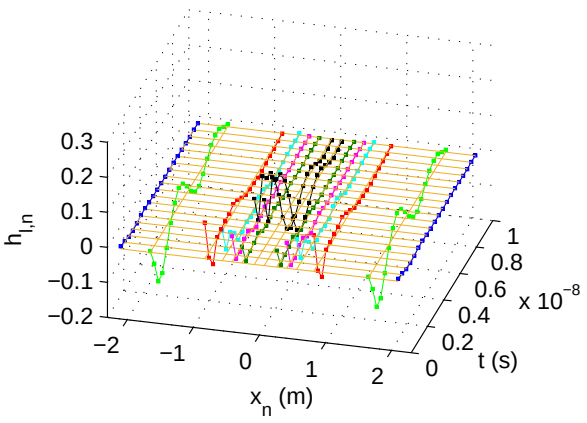

Fig. 10. The optimized FIR filter coefficients for the 14 selected elements for the broadside FI beam pattern.

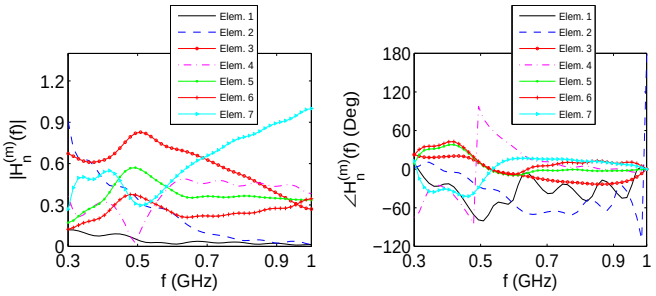

Fig. 11. The transfer functions of the obtained FIR filters for the left 7 elements of the array (the results for the other 7 elements are not shown here since they are symmetrical about the array center for the broadside beam case). (a) Amplitude frequency response, and (b) phase frequency response.

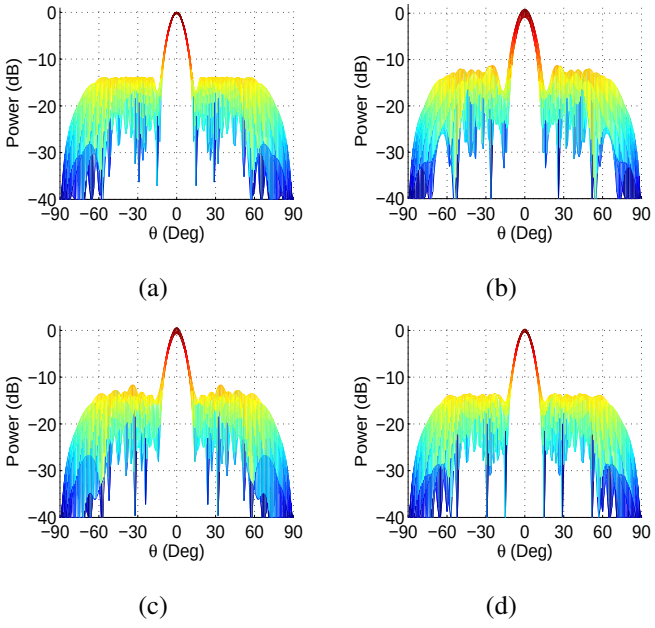

Fig. 12. The synthesized original broadside FI beam pattern shown in (a), and the realized patterns produced by the quantized coefficients shown in (b)-(d) for 5, 6 and 7 bits (all including one sign bit), respectively.

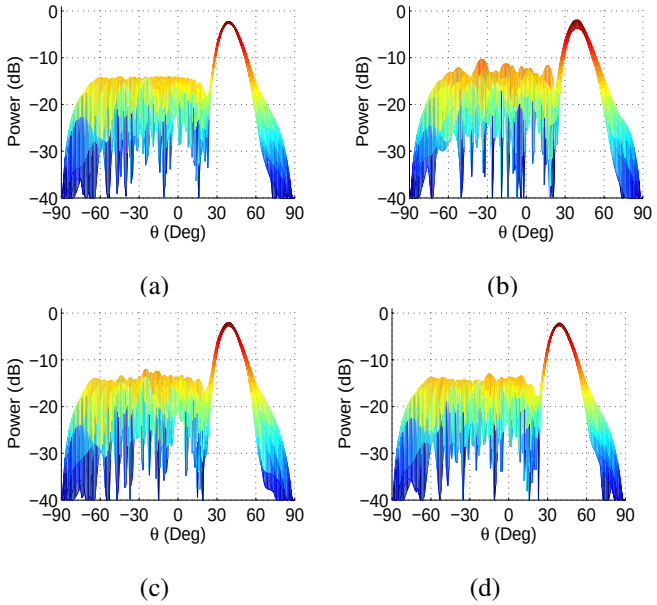

Fig. 13. The original scanned FI beam pattern shown in (a), and the realized patterns produced by the quantized coefficients shown in (b)-(d) for 5, 6 and 7 bits (all including one sign bit), respectively.

IV. Conlusion

A significant extension to the original iterative SOCP synthesis method has been presented to reduce the number of elements for broadband arrays with multiple FI patterns by finding the best common element positions with optimized FIR coefficients. For most cases, it is shown that, by synthesizing discretized multiple cross-over FI patterns, the proposed method can save more elements than the original SOCP that synthesizes a continuously scannable beam pattern. In addition, some complicated space frequency notching can also be incorporated in the proposed synthesis for applications where some powerful interferences exist within a certain frequency band and angular range. The test cases show that the element saving by the proposed method is about $27.27\% \sim 50\%$, depending on the required space coverage range and pattern characteristics such as sidelobe levels and space-frequency notching requirements. The effect of quantizing the FIR coefficients on the performance of the obtained FI patterns is also studied.

It should be noted that the proposed method for synthesizing simultaneous multiple broadband FI beam patterns has a significantly increased computational burden since the number of optimization variables and the number of pattern constraints are raised by a factor of the beam number. Besides, although the obtained minimum element spacings for the synthesized arrays in the examples are larger than or close to half a wavelength at the highest working frequency, the proposed method cannot strictly constrain the minimum element spacing in its optimization process. Further research on the proposed method to realise accurate control of the minimum element spacing would make the method more valuable for practical applications.

REFERENCES

[1] D. B. Ward, R. A. Kennedy, and R. C. Williamson, "Theory and design of broadband sensor arrays with frequency invariant far-field beam patterns," *J. Acoust. Soc. Amer.*, vol. 97, no. 2, pp. 1023-1034, Feb. 1995.

[2] H. H. Chen, S. C. Chan, and K. L. Ho, "Adaptive beamforming using frequency invariant uniform concentric circular arrays," *IEEE Trans. Circuits Syst.*, vol. 54, no. 9, pp. 1938-1949, Sep. 2007.

[3] A. Avokh and H. R. Abutalebi, "Speech enhancement using linearly constrained adaptive constant directivity beamformers," *Appl. Acoust.*, vol. 71, pp. 262-268, 2010.

[4] T. Sekiguchi and Y. Karasawa, "Wideband beamspace adaptive array utilizing FIR fan filters for multibeam forming, " *IEEE Trans. Signal Process.*, vol. 48, no. 1, pp. 274-284, Jan. 2000.

[5] S. Yan, "Optimal design of FIR beamformer with frequency invariant patterns," *Appl. Acoust.*, vol. 67, pp. 511-528, 2006

[6] S. Yan, Y. Ma, and C. Hou, "Optimal array pattern synthesis for broadband arrays," *J. Acoust. Soc. Am.*, vol. 122, no. 5, pp. 2686-2696, Nov. 2007.

[7] D. P. Scholnik and J. O. Coleman, "Optimal array-pattern synthesis for wideband digital transmit arrays," *IEEE J. Selected Topics in Signal Process.*, vol. 1, no. 4, pp. 660-677, Dec. 2007.

[8] E. Mabande, A. Schad, and W. Kellermann, "Design of robust superdirective beamformer as a convex optimization problem," presented at Proc. IEEE Int. Conf. Acoust., Speech, Signal Process. (ICASSP), Taipei, Taiwan, 2009, pp. 77-80.

[9] M. Li, Y. Chang, Y. Li, J. Dong, and X. Wang," Optimal polarised pattern synthesis of wideband arrays via convex optimisation," *IET Microw. Antennas Propagat.*, vol. 7, Iss. 15, pp. 1228-1237, 2013.

[10] W. Liu and S. Weiss, "Design of frequency invariant beamformers for broadband arrays," *IEEE Trans. Signal Process.*, vol. 56, no. 2, pp. 855-860, Feb. 2008.

[11] Y. Zhao, W. Liu, and R. Langley, "Application of the least squares approach to fixed beamformer design with frequency-invariant constraints," *IET Signal Process.*, vol. 5, no. 3, pp. 281-291, 2011.

[12] A. Trucco, M. Crocco, and S. Repetto, "A stochastic approach to the synthesis of a robust, frequency-invariant, filter-and-sum beamformer," *IEEE Trans. Instrum. Meas.*, vol. 55, no. 4, pp. 1407-1415, Aug. 2006.

[13] F. Traverso, M. Crocco, and A. Trucco,"Design of frequency-invariant robust beam patterns by the oversteering of end-fire arrays," *Signal Process.*, vol. 99, pp. 129-135, Jun. 2014.

[14] R. Mars, V. G. Reju, and Andy W. H. Khong, "A frequency-invariant fixed beamformer for speech enhancement," presented at Asia-Pacific Signal and Information Processing Association Annual Summit and Conference (APSIPA), Siem Reap, Cambodia, Dec. 2014.

[15] K.-B. Yu, "Digital beamforming of multiple simultaneous beams for improved target search," presented at IEEE Radar Conference, Pasadena, CA, USA, May 2009, pp. 4-8.

[16] D. Lu, Y. Li, and J. Xiao, "Multi-beam radar search improvement via digital signal re-steering," *International Journal of Design, Anlysis and Tools for Integrated Circuits and Systems*, vol. 2, no. 2, pp. 106-111, Aug. 2011.

[17] V. Murino, A. Trucco, and C. S. Regazzoni, "Synthesis of unequally spaced arrays by simulated annealing," *IEEE Trans. Signal Process.*, vol. 44, no. 1, pp. 119-123, Jan. 1996.

[18] Y. Liu, Z. Nie, and Q. H. Liu, "Reducing the number of elements in a linear antenna array by the matrix pencil method," *IEEE Trans. Antennas Propagat.*, vol. 56, no. 9, pp. 2955-2962, Sep. 2008.

[19] L. Cen, W. Ser, Z. Yu, S. Rahardja, and W. Cen, "Linear sparse array synthesis with minimum number of sensors," *IEEE Trans. Antennas Propagat.*, vol. 58, no. 3, pp. 720-726, Mar. 2010.

[20] G. Prisco and M. DUrso, "Exploiting compressive sensing theory in the design of sparse arrays," presented in IEEE Radar Conference, Kansas City, MO, USA, May 2011, pp. 865-867.

[21] G. Oliveri, M. Carlin, and A. Massa, "Complex-weight sparse linear array synthesis by Bayesian compressive sampling," *IEEE Trans. Antennas Propagat.*, vol. 60, no. 5, pp. 2309-2326, May 2012.

[22] M. D. Gregory and D. H. Werner, "Ultrawideband aperiodic antenna arrays based on optimized raised power series representations," *IEEE Trans. Antennas Propagat.*, vol. 58, no. 3, pp. 756-764, Mar. 2010.

[23] M. D. Gregory, F. A. Namin, and D. H. Werner, "Exploiting rotational symmetry for the design of ultra-wideband planar phased array layouts," *IEEE Trans. Antennas Propagat.*, vol. 61, no. 1, pp. 176-184, Jun. 2013.

[24] J. H. Doles, III, and F. D. Benedict, "Broad-band array design using the asymptotic theory of unequally spaced arrays," *IEEE Trans. Antennas Propagat.*, vol. 36, pp. 27-33, Jan. 1988.

[25] M. Crocco and A. Trucco, "Stochastic and analytic optimization of sparse aperiodic arrays and broadband beamformers with robust superdirective patterns," *IEEE Trans. Audio, Speech Lang. Process.*, vol. 20, pp. 2433-2447, Nov. 2012.

[26] Z. Li, K. F. Cedric Yiu, and Z. Fen, "A hybrid descent method with genetic algorithm for microphone array placement design," *Applied Soft Computing*, vol. 13, pp. 1486-1490, 2013.

[27] M. B. Hawes and W. Liu, "Robust sparse antenna array design via compressive sensing," presented at International Conference on Digital Signal Processing, Fira, Greece, Jul. 2013.

[28] M. B. Hawes and W. Liu, "Sparse array design for wideband beamforming with reduced complexity in tapped delay-lines," *IEEE Trans. Audio, Speech Lang. Process.*, vol. 22, no. 8, pp. 1236-1247, Aug. 2014.

[29] Y. Liu, L. Zhang, C. Zhu, and Q. H. Liu, "Synthesis of nonuniformly spaced linear arrays with frequency-invariant patterns by the generalized matrix pencil methods,", *IEEE Trans. Antennas Propagat.*, vol. 63, no. 4, pp. 1614-1625, Apr. 2015.

[30] C. Zhu, X. Li, Y. Liu, L. Liu, and Q. H. Liu, "An extended generalized matrix pencil method to synthesize multiple-pattern frequency-invariant linear arrays," *IEEE Antennas Wireless Propag. Lett.*, vol. 16, pp. 2311-2315, Jun. 2017.

[31] Y. Liu, L. Zhang, L. Ye, Z. Nie, and Q. H. Liu, "Synthesis of sparse arrays frequency-invariant-focused beam patterns under accurate sidelobe control by iterative second-order cone programming," *IEEE Trans. Antennas Propagat.*, vol. 63, no. 12, pp. 5826-5832, Dec. 2015.

[32] E. J. Candes, M. B. Wakin, and S. P. Boyd, "Enhancing sparsity by reweighte $\ell 1$ minimization," *Fourier Anal Appl.*, vol. 14, pp. 877-905, Dec. 2008.

[33] J. F. Sturm, "Using SeDuMi 1.02, a MATLAB toolbox for optimization over symmetric cones," *Optim Method Softw.*, vol. 11, pp. 625-653, 1999.